JOURNAL OF MATERIALS SCIENCE 30 (1995) 4233–4243

# Investigation of complex failure modes in fibre bundles during dynamic mechanical testing using acoustic emission and Weibull statistics

E. U. OKOROAFOR, R. HILL*
*Centre for Research in Materials Science and Engineering, Department of Chemistry and Physics, The Nottingham Trent University, Clifton Campus, Nottingham NG11 8NS, UK*

Mechanical strength studies have been carried out on fibre bundles used in composite manufacture. Logarithmic Weibull plots derived from dynamic fibre bundle tensile tests, involving acoustic emission (AE) techniques are not linear over the entire fibre bundle failure strain range. This makes it impossible to use the two-parameter Weibull strength distribution function to describe fully a fibre bundle response in dynamic situations. The plots exhibit portions of different slopes, with no sharp boundaries demarcating them. This is attributed to the overlapping of the various fibre failure modes occurring with increasing fibre bundle strain. AE event–strain (fibre failure) analysis showed that with increasing strain, the fibre failure mode changes from predominantly singlets (a single-fibre failure at a time) to doublets (simultaneous failure of two fibres), and then higher multiple fibre failure modes. The various failure modes overlap about the maximum fibre bundle stress, and each multiple fibre failure mode contributes towards the combined Weibull plot with a slope of the corresponding multiple of the slope due to the singlet fibre failure mode. In the light of these observations, we have modified the two-parameter Weibull function, which is valid only when singlets are dominant, to include contributions from higher order fibre failure modes for a better description of fibre bundles dynamic stress–strain responses. The fit between theory and experimental data appears to confirm the role played by the higher order fibre failure modes in changing the slope of the Weibull plots and in defining the shape of the fibre bundle stress–strain response, particularly about and beyond the maximum bundle stress position.

## 1. Introduction

The testing of complete fibre bundles has gained increased support [1–6] in recent years, because the statistical data concerning fibre strength are much more conveniently obtained using complete fibre bundles and, also the data are more representative of the situation which prevails in a finished fibre-reinforced composite material. Information regarding the state of a fibre bundle (the number of failed fibres) can be extracted using mechanical testing, possibly including the measurement of acoustic emission (AE) events, which with suitable adjustment can give accurate and automatic information on the extent of fibre failures. The fibre strength distribution has usually been described using a two-parameter Weibull distribution function [7], which for uniform extension of a number, $N_0$, of fibres of normalized length, $L$, the number, $N_s$, surviving at strain $\varepsilon$, and assuming dominance of singlet fibre failures, can be expressed as

$$N_s = N_0 \exp[-L(\varepsilon/\varepsilon_0)^m] \quad (1)$$

with $m$ and $\varepsilon_0$ commonly referred to as the Weibull shape and strain-scale parameters or as the strength distribution parameters. $(\varepsilon/\varepsilon_0)^m$, is the distribution function and $L(\varepsilon/\varepsilon_0)^m$ the expected average number of defects for a failure strain less than $\varepsilon$ in a Weibull fibre bundle of length $L$. When load, $F$, is equally shared by the surviving fibres, the stress–strain relationship is expressed as

$$\sigma = E_f \varepsilon \exp[-L(\varepsilon/\varepsilon_0)^m] \quad (2)$$

$E_f$ is the fibre modulus and $\sigma(F/AN_0)$, represents the nominal stress. The Weibull shape parameter, $m$, is obtained from the slopes of the logarithmic Weibull plots produced in the form, $\ln\ln(\varepsilon E_f/\sigma)$ versus $\ln(\varepsilon)$ and/or $\ln\ln(N_0/N_s)$ versus $\ln(\varepsilon)$, derived

* Author to whom all correspondence should be addressed.

0022–2461 © *1995 Chapman & Hall*

from the tensile stress–strain response and or the AE event–strain response. The linearity of such Weibull plots over the entire strain range indicate that a Weibull treatment is applicable and also confirms the dominance of singlet fibre failure mode.

Cowking *et al.* [1], in testing E-glass fibre bundles, obtained linear Weibull plots over the entire strain range. The data, however, in their paper were taken using more time-consuming quasi-static tensile testing which, as they reported, resulted in singlet fibre failures over the fibre bundle failure strain range. Surprisingly, the shape of their fibre bundle load–strain response, particularly beyond the maximum load position, indicated significant load drops which would not seem to agree with a dominance of singlet fibre failure mode. Employing similar experimental conditions, Hamstad and Moore [2], using fibre bundles of Kevlar-49, reported that about 70% of the fibres failed in the singlet mode and the rest failed in higher order modes. Chi *et al.* [3], also carried out tests on carbon fibre bundles to obtain the fibre system strength distribution parameters. Their attempts to simulate the fibre systems load–strain response from Equation 2, using their values for $m$ and $\varepsilon_0$, proved futile, particularly for load/strain values about the fibre bundle maximum load, because of an inability to take into consideration the changing slope of the Weibull plot, which indicated changing Weibull shape parameter, $m$. The value of the parameter $m$ used in their simulation was that obtained from the average slope of their Weibull plot. They pointed out, however, that the disagreement between theory and experiment near the maximum load position, could be due to multiplet failure of fibres and the inability of the Weibull function to account for this. Other work by us [8] carried out on fibre bundles, has indicated that only values of the Weibull shape parameter, $m$, obtained from the low-strain regions of the Weibull plots are in agreement with those obtained from single-fibre tests [9]. This suggests a dominance of singlet fibre failures at low strains during bundle tests. In addition, we showed that such values of $m$ and the associated strain-scale parameter, $\varepsilon_0$, could only be used with Equation 2 to simulate the early load–strain response of the fibre bundle in dynamic tensile tests. At about and beyond the maximum load position, the two-parameter Weibull treatment proved inadequate.

The present work represents an attempt to find a better means of obtaining the statistical parameters used to describe the strength distribution of a fibre system. The requirement is that the tests should use a constant crosshead speed, which would allow measurements to be undertaken in a shorter time, but with the Weibull plots diverging from linearity at higher strains, and account could be taken of this. Both tensile testing and AE techniques were employed to elucidate the origin of the divergence from linearity in the Weibull plots. This has been taken into account in attempts to modify Equations 1 and 2 to provide a fuller description of the fibre bundle stress–strain response.

## 2. Experimental procedure

### 2.1. Fibre bundle specimen preparation

Fibre systems used in this study included Kevlar-49 (Dupont (UK) Ltd; Den 2160, Dtex 2400, 1000 filaments, finish-free) and E-glass (Fibre-Glass (UK) Ltd; Equerove, Silane-sized, EC13, 600 Tex). Fibre bundles cut from the "cakes" were laid across the gap between two aluminium plates, and after taking care that the fibres were parallel, the regions outside the fibre bundle specimen gauge length were then bonded to the aluminium plates using Ciba-Geigy Araldite S2.

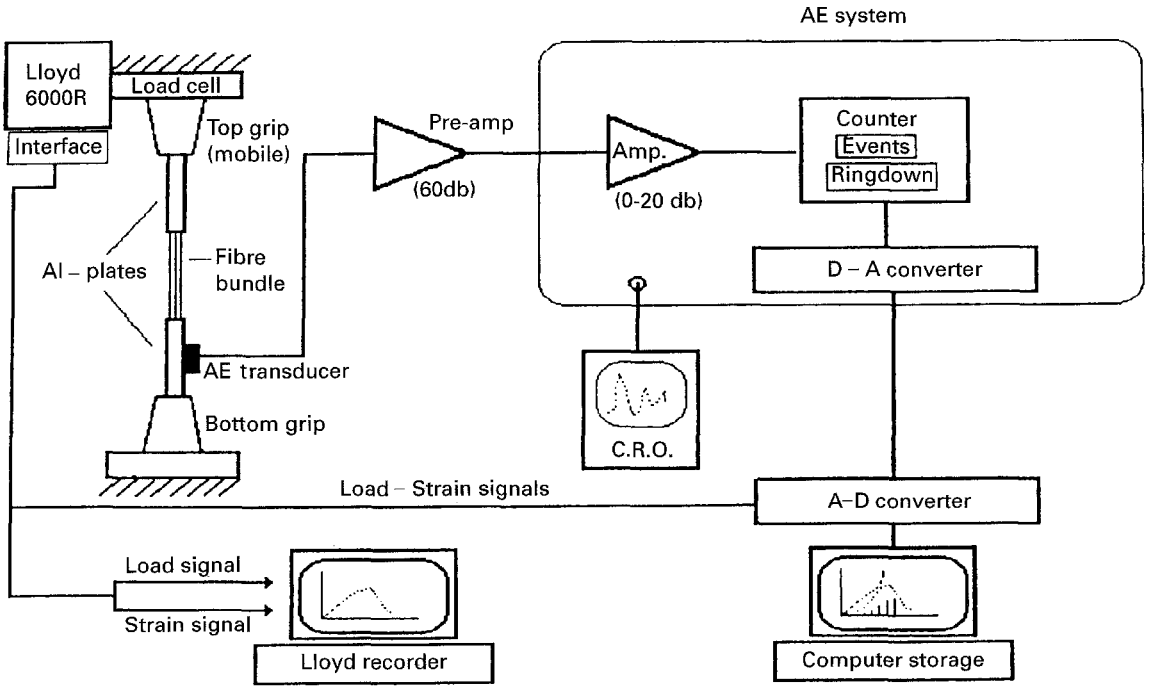


*Figure 1* Schematic diagram of the experimental measurement system.

## 2.2. Test conditions

Before testing, the as-received fibre bundle specimens were lubricated with silicone oil to minimize interfibre friction, which induces cooperative fibre failure by friction-induced load transfer, and consequently reduces bundle strength [8]. This friction also generates interfibre noise, causing spurious AE. During testing, the aluminium end-plates were carefully mounted in the grips of the Lloyd-6000R tensile testing machine. The gauge length of the fibre bundle specimens throughout the tests was 70 mm. Tensile tests to failure were carried out at a constant crosshead movement rate of 0.08% $min^{-1}$.

Acoustic emission (AE) from fibre failure was monitored during the tests to verify the mode of fibre failure within the bundles (i.e. whether singlets, doublets, triplets, etc.), which would modify the stress–strain response. Another objective in using AE was to consider a suitable AE parameter for predicting failure or the residual life of the fibre bundles. For the tests, a commercial AE sensor (Acoustic Emission Technology Corporation, type AC375L, resonant frequency 375 kHz) was utilized. This transducer was spring clamped to the aluminium end-plate of the test specimen mounted in the bottom grip of the tensile machine. Silicone grease was used as an acoustic couplant. The AE signals from the transducer, in the form of decaying sine waves of given initial amplitude, frequency and decay constant, were preamplified by 60 dB, using a preamplifier with narrow band filtering around the transducer resonance (AECL 2100 preamplifier), and further processed using the AECL 2100M acoustic emission system. The processed data were then passed via an integral analogue-digital (A–D) board to a computer which stored the AE event numbers (fibre failure numbers), the corresponding ringdown counts (number of positive threshold crossings of the decaying signal) per event or group of events, the strain and load values. The system (A–D board and computer) was configured so that by sensing increments in event numbers and increments in ringdown counts, it was possible to quantify AE events in terms of ringdown count per event, $N_e$, and fibre failure mode. The ringdown counts per event figures were limited by the speed of the A–D processor, but it still provided an effective method of AE quantification. The ringdown counts can be looked upon as being related to the energy released by the failing fibres because they are associated with the acoustic energy released by the fibre failure events. AE instrument settings were: dead time 0.2 ms, and threshold 0.2 V. The latter was chosen to minimize electronic background noise, noise from the grips and from the tensile testing machine, thus ensuring that received signals were from the fibre failures in the bundles. Note also, that, as the AE signal duration is enhanced by stress-wave reflection within the specimen/support system [10], the attachment of the AE sensor to the aluminium end-plate mounted in the immobile bottom grip of the tensile machine, was found to dampen the AE signals more rapidly. Fig. 1 shows a schematic diagram of the experimental system.

## 3. Results and discussion

The data in Figs 2–5, apply to tensile testing to failure of fibre bundles of as-received Kevlar-49 and E-glass fibre systems. Fig. 2a and b, show the tensile stress–strain curves, the AE cumulative events (continuously rising curve) and the corresponding ringdown counts per event, $N_e$, as the Kevlar-49 and E-glass fibre bundles, respectively, are taken to failure. It can be seen, from the maximum bundle stress, $\bar{\sigma}_{max}$, that Kevlar-49 is stronger than E-glass. Using the AE cumulative event count as an indication, fibre failure started earlier for E-glass (approximately at $\varepsilon \approx 1\%$), compared to Kevlar-49 ($\varepsilon \approx 1.8\%$). The strain values at maximum bundle stress, which we term $\bar{\varepsilon}_{0max}$, followed the same trend (for E-glass, 2.3%; for Kevlar-49, 2.45%) perhaps indicating a relationship between the commencement of fibre bundle failure and the bundle failure strain. In the case of Kevlar-49, most of the fibres in the bundle failed around the maximum stress position, indicating a narrower strength distribution than for E-glass.

Inspection of the evolution of the ringdown counts per event from the events in Fig. 2a and b show clearly that this parameter rises during the tests but with large fluctuations. This rise in the ringdown count is associated with a rise in the amount of acoustic energy released by the fibre failure events and can be related to the fibre failure stress [11]. This rise in $N_e$ also gives an associated rise in such AE parameters as event amplitude and event duration (assuming no event overlap occurs). At about the maximum stress position, it can be seen that saturation of the ringdown counts occurs. However, the general trend exhibited by the ringdown count with strain shows that it may be possible to correlate an AE signal parameter to the maximum fibre (failure) stress. In a previous publication [12], ringdown counts were used to monitor subtle changes in the strength of surface-treated fibre bundles and also the extent to which the fibres in the bundle maintain their individuality after such treatments. In the latter situation, when there are events with ringdown counts much less than those emanating from fibre failure events, these were clearly associated with the cracking or tearing of the surface materials binding the fibres together, and indicated the loss of individuality of the fibres in the bundle after the surface treatment. In general, the average ringdown count for the fibre failure events decreased as the average fibre bundle strength decreased.

Fig. 3a and b, show the logarithmic Weibull plots derived from the tensile stress–strain and AE event–strain data of Fig. 2a and b. While the Weibull plots are not linear over the fibre bundle failure strain range, it is important to point out that these plots derived from both testing techniques shadow each other closely: a clear indication that the AE output, to a large extent, followed the fibre failures in the bundles over the entire strain range. When the Weibull shape parameter, $m$, which describes the fibre strength distribution, is obtained from the slope of linear Weibull plots (Fig. 3a and b), it is obvious that the slope changes with strain and, as such, a single shape parameter would be inadequate to describe fully this

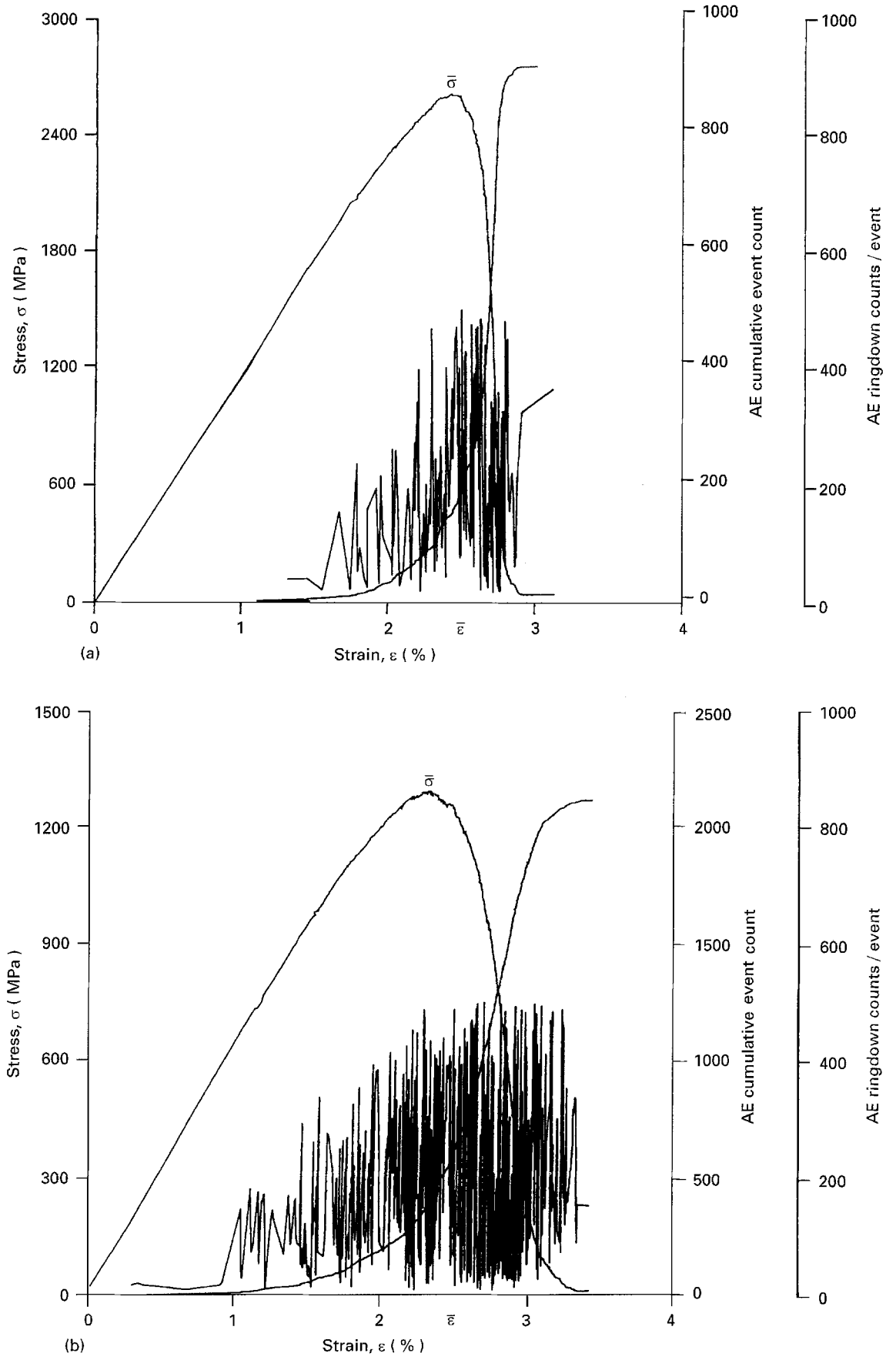


*Figure 2* Tensile stress–strain curves (rising from zero strain), the AE cumulative events and the corresponding ringdown count per event (irregular graph), as (a) Kevlar-49, and (b) E-glass fibre bundles are taken to failure.

behaviour. One might say that the plots exhibit two regions of linearity separated by the region of the average bundle failure strain. The value of the Weibull shape parameter, $m_2$, obtained from the high-strain region is large (steeper slope) compared to the value, $m_1$, obtained from the low-strain region. These values of $m$, the associated Weibull strain-scale factors ($\varepsilon_{01}$ and $\varepsilon_{02}$) and the tensile properties of the fibre systems

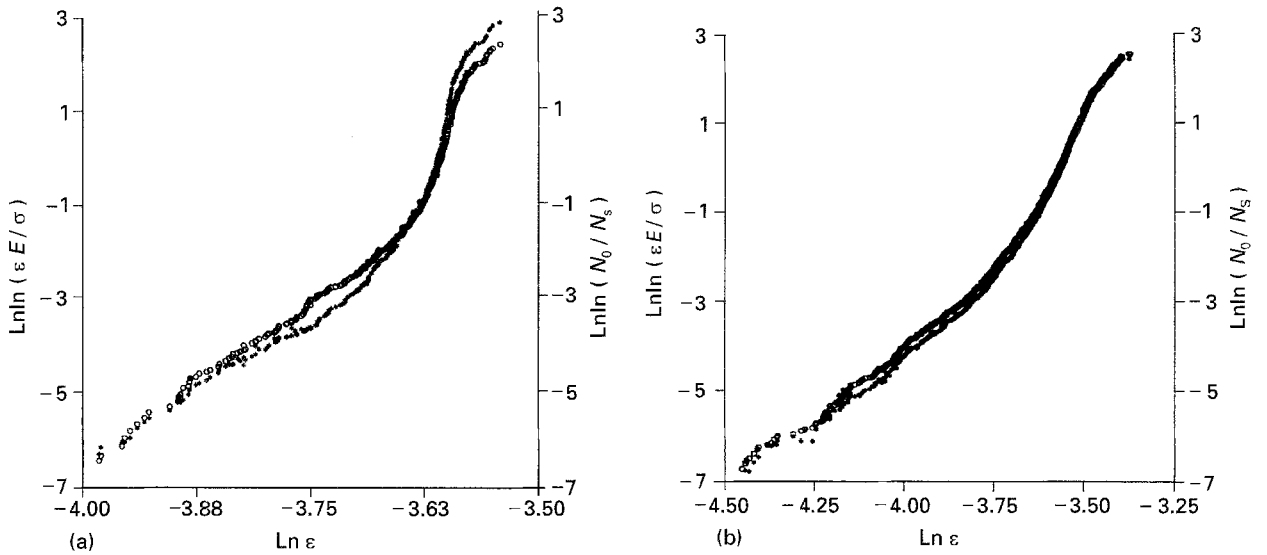


*Figure 3* Weibull logarithmic plots derived from the (*) tensile stess–strain and (○) AE event–strain data in Fig. 2, for (a) Kevlar-49, and (b) E-glass fibre bundles.

TABLE I Tensile properties of Kevlar-49 and E-glass fibre bundles, and their Weibull strength distribution parameters obtained at both low and high strains in taking the bundles to failure by continuous straining

| Fibre system | Elastic modulus $E$ (GPa) | Bundle strength $\bar{\sigma}$ (MPa) | Failure strain $\varepsilon$ (%) | Weibull parameters | | | |
|---|---|---|---|---|---|---|---|
| | | | | Low ($\varepsilon$) | | High ($\varepsilon$) | |
| | | | | $m_1$ | $\varepsilon_{01}$ | $m_2$ | $\varepsilon_{02}$ |
| Kevlar | 117 | 2600 | 2.45 | 14.1 | 2.96 | 45.5 | 2.66 |
| E-glass | 65.7 | 1305 | 2.31 | 6.7 | 3.07 | 18.3 | 2.71 |

under consideration are given in Table I. Note, that both values of $m$ obtained for Kevlar-49 are larger than those obtained for E-glass, confirming that Kevlar-49 always has a narrower strength distribution. Previous studies [8], however, showed that $m_1$, obtained from the low-strain region of the Weibull plots, agreed with those obtained by earlier workers employing either the single-fibre testing technique [9] or the quasi-static mechanical fibre bundle testing technique [1]. This suggests that singlet fibre failure mode is dominant at low strains. Therefore, this allows the large values of $m_2$, obtained at high strains to be associated with the presence of higher order fibre failure modes, which must be accounted for in a fuller description of the fibre bundle response during dynamic tests. This multiplet failure at high strains can be looked upon as a step in the increasing complexity which takes place in moving from a single-fibre test to a fully developed resin/fibre composite where multiplet fibre fractures may precede the failure of the composite as a whole.

## 3.1. Multiplet fibre failure

In Fig. 4a and b, the tensile stress–strain and the AE event–strain data presented in Fig. 2a and b are replotted, and include the fibre failure modes (singlets, doublets, triplets, etc.). Multiplets are detected by the rise in the AE event counts in the time the electronic measurement system requires before reading of the next event count value. Multiplets are apparent in the step-up of the AE event count present in the data file generated during the test. A high-speed computer interface is used to minimize effects associated with the speed of interface addressing. Confirmation of the physical reality of multiplets is confirmed by the divergence from a single-parameter Weibull plot and the coincidence of theory and experiment when multiplet failure is assumed.

Fig. 4a and b clearly show the dominance of the singlet fibre failure mode at low strains. As the average bundle failure strain is approached, the doublet fibre failure mode appears, overlapping with the singlets. With increasing bundle strain, higher order fibre failure modes appear, overlapping also with the lower order modes. The high-order multiplets appear in the region of most rapid load drop and bundle failure. When most of the fibres in the bundle had failed, singlet failure once again become predominant.

Using the fibre failure modes as an indication, the first few doublets in both fibre systems, appeared at about 85% of the average maximum bundle stress, and coincided with the point where the bundle stress–strain response showed significant deviations from linearity and the AE event count rate showed a rapid increase (see Fig. 2). It is possible that this is a clear indication of the imminence of failure of the fibre bundle as a whole. In fact, with only about 5% of the fibres in the bundle having fractured and in view of

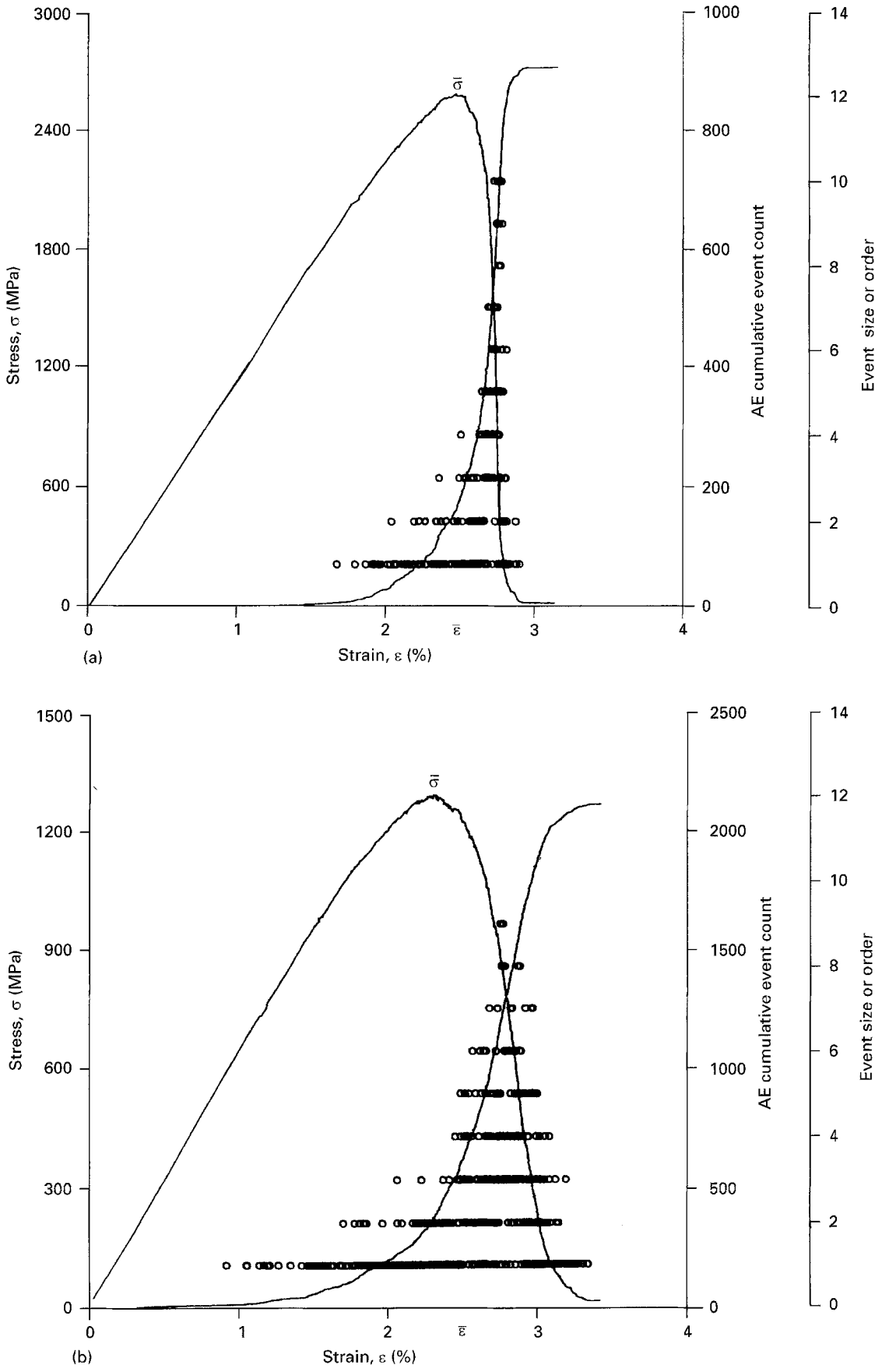


*Figure 4* Replots of the data in Fig. 2 for testing to failure of (a) Kevlar-49, and (b) E-glass fibre bundles, and including the distribution of fibre failure multiplets: singlet, event size = 1 (lowest distribution positioned by strain); doublet, event size = 2 (next lowest distribution, etc.); triplet, event size = 3; etc.

the statistical nature of fibre strength, one could argue here that the bundle stress at the first few occurrences of the doublet fibre failure mode, is a conservative estimate of the fibre strength.

Extending such an argument to unidirectional composites is not unreasonable, because fibres constitute the major load-bearing component, and their strength, to a large extent, determines the tensile

strength of the composite. This experimental observation lends some degree of support to the theoretical work of Zweben and Rosen [13], who carried out parametric analysis of three-dimensional composite failure only to the first appearance of doublets, and proposed, using the corresponding stress, a conservative estimate of the strength of the composite. It can be argued that the mechanisms of doublet generation in fibre bundles and the finished composite are related.

In uniaxially reinforced composites, for instance, it has been suggested [14] that as tensile load increases, isolated fibre failures (singlets) occur at locations of particularly weak spots. Such isolated fibre failures do not normally cause composite failure because the matrix transfers the load from the failed fibre to the segments of its neighbours in the break plane and back again into the fibre some distance from the break. As the load increases, the number of singlets increases, and eventually the overloaded segment of a fibre adjacent to a singlet will be abnormally weak and therefore will fail simultaneously with the singlet, resulting in a double failure (doublet). The process continues, generating more and higher order-multiplets until one multiplet reaches a critical size and failure of the composite as a whole ensues. For our fibre bundle tests, it is possible that the dynamic nature of the experiments ensures that, as load increases, and after a certain number of singlet fibre failures, the excess load is not equally redistributed among the remaining fibres in the bundle and the overloaded fibres adjacent to a singlet would fail at the same time as the singlet or nearly so, giving doublets, triplets, etc., depending on the situation. This might be the major difference between our experimental approach to testing fibres and the quasi-static test procedure undertaken by Cowking *et al.* [1]. In the latter method, it is possible that load is equally shared in any configuration of failed and surviving fibres, hence minimizing multiplet fibre fractures.

It is clear from Fig. 4a and b, that the manner in which the different fibre failure modes appeared, could throw light on both the evolution of the ringdown counts with strain as shown in Fig. 2a and b, and the non-linearity of the Weibull plots, shown in Fig. 3a and b. In the case of the ringdown counts, it is possible, due to the occurrence and overlap of the various fibre failure modes at high strains, that significant overlap of AE signals begins to occur. This will result in lower values of the ringdown counts than might be expected and explain the fact that this parameter saturates. This is discussed in Section 4. The appearance of the multiplet fibre failure modes at high strains would effectively make the Weibull plots steeper in this strain region, hence the non-linearity of these plots over the fibre bundle failure strain range. In addition, the overlapping of the various fibre failure modes about the maximum stress position ensures there is no sharp boundary separating the low and the high strain regions of the Weibull plots. At high strains, there is a continuous increase in the steepness of the plots with strain. In this region, the slope, $m$, of the Weibull plot, is not a direct multiple of the value $m$ obtained at low strains.

The manner by which the fibre failure modes affect the Weibull plots is shown in Fig. 5a and b, where, in each case, the Weibull plots derived from the singlet, doublet, and triplet fibre failure modes are shown, combined with Weibull plot for all failure modes. While the combined plots are of $\ln\ln(N_0/N_s)$ versus $\ln(\varepsilon)$, with $N_0$ representing the original number of fibres in the bundle, and $N_s$ the number surviving at strain $\varepsilon$, the plots involving the individual fibre failure modes are of $\ln\ln(N_{0i}/N_{si})$ versus $\ln(\varepsilon)$. $N_{0i}$, is the number of fibres that failed in the mode $i$ over the fibre bundle failure strain range and $N_{si}$, the number surviving at strain $\varepsilon$ and $c_i$, the concentration at strain $\varepsilon$, relative to $N_0$, of the fibres that have failed. These plots show clearly the already established fact that singlets are dominant at low strains and the slope of the logarithmic plot in this strain region is $m$. Doublets are practically absent at low strains, but as strain rises (i.e. about the maximum stress position), they appear and their number increases rapidly, hence contributing a slope of 2 $m$ to the combined plot. The triplets appear also at high strains, with their number increasing with strain and contributing a slope of 3 $m$ to the combined Weibull plot. Because each multiplet fibre failure mode contributes towards the combined plot, a slope that is the corresponding multiple of the slope $m$ due to the singlets, then $m$ must be the natural Weibull shape parameter of the fibre system under investigation. Higher values of $m$ result from higher values of load applied to the bundle.

These data show that it is not necessary to have singlet fibre failure mode only in order to determine $m$. The value of $m$ can be determined from any multiplet fibre failure mode, as long as the mode can be identified, with acoustic emission used to achieve this.

It is clear from the Weibull plots of Fig. 5, which show the singlet, doublet, and triplet fibre failure modes, that a combination, over the entire fibre bundle failure strain range, of such plots for all the observed fibre failure modes would fully reproduce the combined plot. Thus, at any strain $\varepsilon$, the combined plot can be defined as

$$\ln\ln(N_0/N_s) = \ln[\Sigma c_i \ln(N_{0i}/N_{si})] \quad (3)$$

and with

$$\ln(N_{0i}/N_{si}) = L(\varepsilon/\varepsilon_{0i})^{im} \quad (4)$$

derived from Equation 1, the number of fibres in the bundle surviving at strain $\varepsilon$ can be expressed as

$$N_s = N_0 \exp[-L\Sigma c_i(\varepsilon/\varepsilon_0)^{im}] \quad (5)$$

and the corresponding stress–strain relationship expressed as

$$\sigma = E_f \varepsilon \exp[-L\Sigma c_i(\varepsilon/\varepsilon_0)^{im}] \quad (6)$$

where $E_f$ is the fibre modulus and $im$ and $\varepsilon_{0i}$ the Weibull shape and strain-scale parameters, respectively, for the fibre failure mode $i$. As the average fibre bundle failure strain, $\varepsilon_{AV}$ is determined by the various

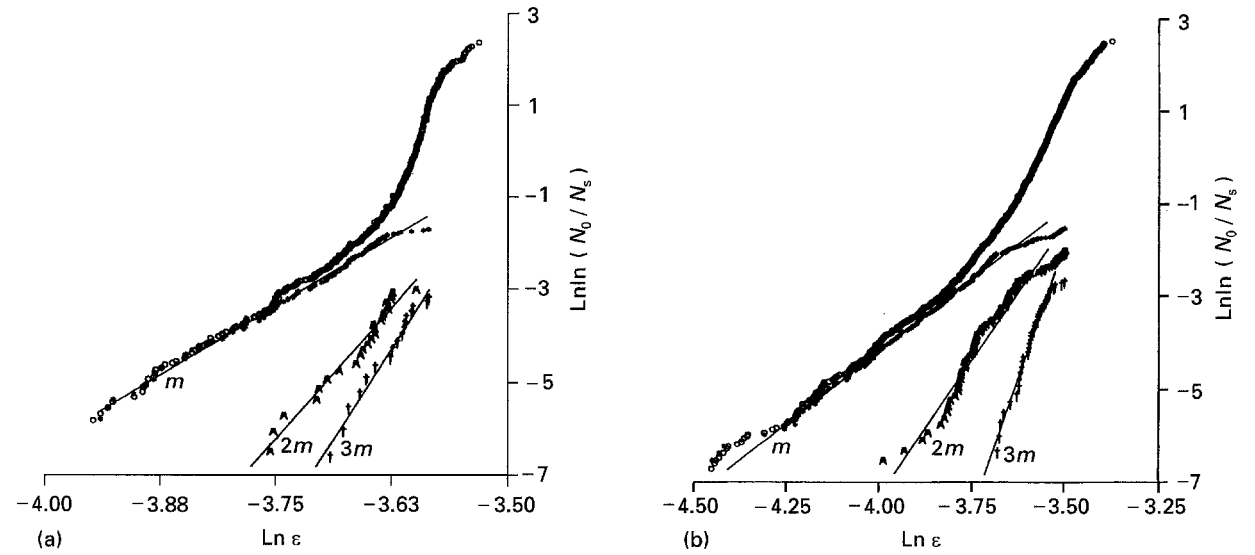


*Figure 5* Weibull logarithmic plots derived from the AE event–strain data for (a) Kevlar-49, and (b) E-glass, fibre bundles, and showing the contributions from the singlet, doublet and triplet fibre failure modes.

fibre failure modes in operation during the tests, the Weibull strain-scale parameter can be defined as

$$\varepsilon_{0i} = \varepsilon_{AV}(im^{1/im}) \quad (7)$$

In Fig. 6a and b, the tensile stress–strain responses of fibre bundles of Kevlar-49 and E-glass, respectively, are compared to those simulated using Equation 6. The variables $c_i (i = 1, 2, 3, \ldots,)$, were obtained via AE measurements. It is evident from Fig. 6, that there is very good agreement between the simulated and experimental curves. This confirms the validity of Equations 3–7, and thereby reveals the significant role played by the multiple fibre failure modes in defining the shape of the fibre bundle dynamic tensile stress–strain response, particularly about and beyond the bundle maximum stress position. Beyond the maximum stress position, the higher order fibre failure modes lead to large load drops which the Weibull parameters determined at low strains ($m_1$ and $\varepsilon_{01}$, due to singlets), cannot describe.

## 3.2. Saturation of ringdown counts per event

As a resonant transducer was used in this study, the electrical signal produced is not an exact analogue of the original stress wave. Subject to a single stress pulse, the AE transducer will oscillate in a damped sinusoidal manner so that the voltage, $V_t$, at the transducer at a time $t$ after an initial pulse is given by

$$V_t = V_0 \exp(-\beta t)\sin(\omega t) \quad (8)$$

where $V_0$ is the maximum initial transducer signal voltage, $\beta$ is the damping constant and $\omega$ the angular transducer frequency. Fig. 7a, shows schematically an idealized ringdown of the transducer that would be expected from a single AE event, and some of the possible AE signal parameters ($V_0$ = initial transducer voltage amplitude; $t_d$ = AE event duration; with $N_e = 8$, the ringdown counts per event) that could be related to the nature of the event. It can be seen that the values obtained for these AE parameters are dependent on the threshold voltage $V_{th}$. By lowering the threshold voltage, the event duration recorded will be increased and, consequently, the ringdown counts per event $N_e$. The ringdown count, $N_e$ is given by

$$N_e \sim t_d/T \quad (9)$$

where $T$ is the period of the oscillations. As the last oscillation above $V_{th}$ is an integral number of wavelengths from the origin, we have

$$V_{th} = V_0 \exp(-\beta N T) \quad (10)$$

in which case, the ringdown count recorded for a single AE event is

$$N = 1/(\beta T)\ln(V_0/V_{th}) \quad (11)$$

This relationship shows that if $V_0$ is proportional to the fibre failure stress, $\sigma_f$, then $N_e$ is proportional to $\ln(\sigma_f)$.

Considering two identical AE stress pulse events separated in time of arrival at the transducer by $\Delta t$, where $\Delta t$ is such that the signals are in phase and overlapping, then a waveform similar to that shown schematically in Fig. 7b results. In this case, the number of ringdown counts can be expressed as

$$N \sim t'_d/T \quad (12)$$

where $t'_d$, is the combined event duration, containing information which can be related to $\Delta t$. It is clear from Fig. 7b that $t'_d$ would decrease as $\Delta t$ becomes smaller, and vice versa. This illustrates the relative dependence of the ringdown counts, $N_e$, on the interval of time between events. When $\Delta t = 0$, then $N$ would be comparable to that from a single event and, in this situation, the initial amplitude of the signal would be a better indicator of the event amplitude rather than the ringdown counts. In reality, $\Delta t$, fluctuates and the parameter $N_e$ for multiplet events does not depend only on $\Delta t$, but also on the initial amplitude and frequency of the individual event signals constituting the fibre fracture multiplet. The signal phase

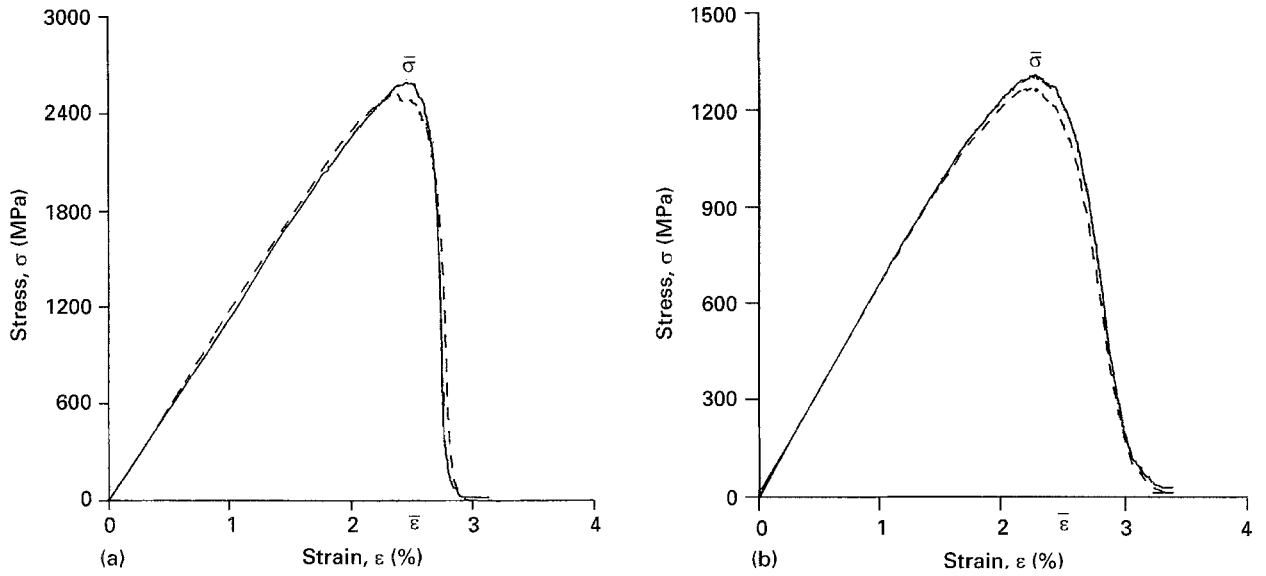


*Figure 6* Comparison of the (——) experimental and (- - - - -) simulated tensile stress–strain responses of (a) Kevlar-49, and (b) E-glass fibre bundles. The simulation employed Equation 6.

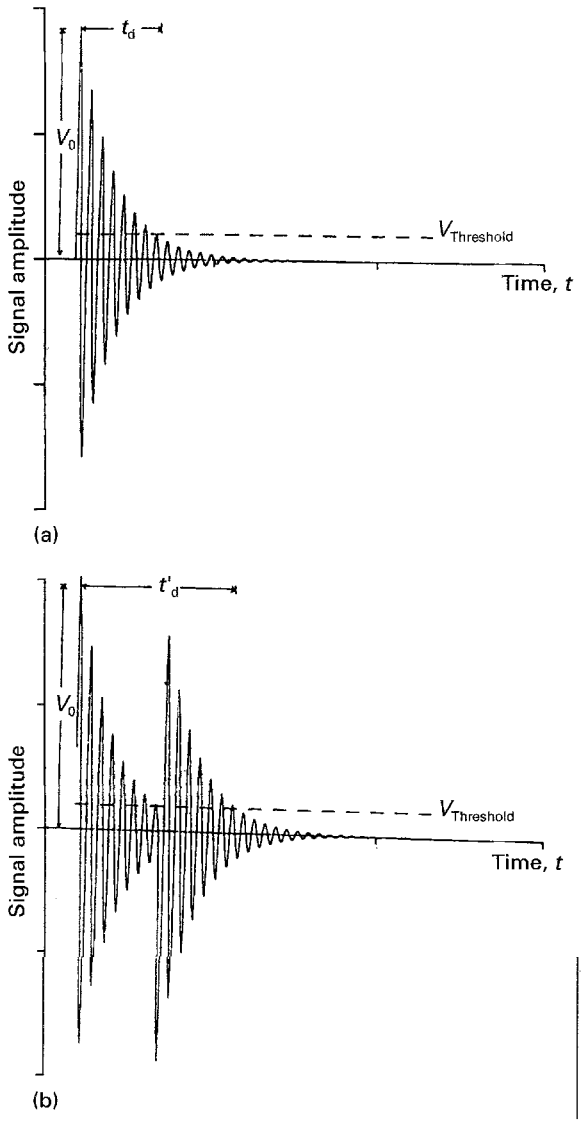


*Figure 7* Schematic idealized ringdown signals produced by an AE transducer in response to (a) a single-pulse event, and (b) simultaneous double-pulse events, and showing such AE signal parameters as amplitude, $V_0$, threshold voltage, $V_{th}$, the respective event duration and ringdown counts: (a) $t_d$ and $N = 8$; (b) $t'_d$ and $N = 15$.

determines whether signal interference is constructive or destructive. The latter situation would reduce $N_e$. These factors, and possible energy loss factors, such as creation of new fracture surfaces, acoustic reflection at interfaces and boundaries, signal attenuation in transit to the measuring transducer, and the rate at which the stored elastic energy is released in the failure process, play a significant role in the value of $N_e$. Thus, while $N_e$, in general, is expected to increase with rising fibre failure stress and thus differentiate fibre failure stress, it could also exhibit large fluctuations. This is clear from the experimental data presented.

Another disturbing factor in measuring $N_e$ is the role of the AE equipment in defining an AE event. In the experimental arrangement used, an AE event is defined as an isolated transducer signal, separated from the other signals by a period of time during which no threshold crossings occur. This period is preset at 200 μs (which is about 75 transducer oscillation periods for the transducer resonant frequency of 375 kHz). For a group of events to be treated as a singlet by the measurement system used, it is necessary that the period between the nearest ringdown peaks (above the threshold) of adjacent signals does not exceed the preset time for event discrimination, or else the events would be recorded as singlets.

With these aspects of the AE technique in mind, the ringdown counts saturation observed during testing can be considered. At low strains, singlets were predominant and the observed ringdown counts for the fibre failure events, as expected, showed a general increase with fibre failure stress or strain consistent with the arriving AE signals being isolated (Fig. 2). This was not the case at higher strains where we observed a rapid increase in the fibre failure rate and some overlapping of the various fibre failure modes might be expected. At high strains, the smaller than expected values obtained for the ringdown counts per event and the apparent saturation of this parameter might be attributed to the following factors:

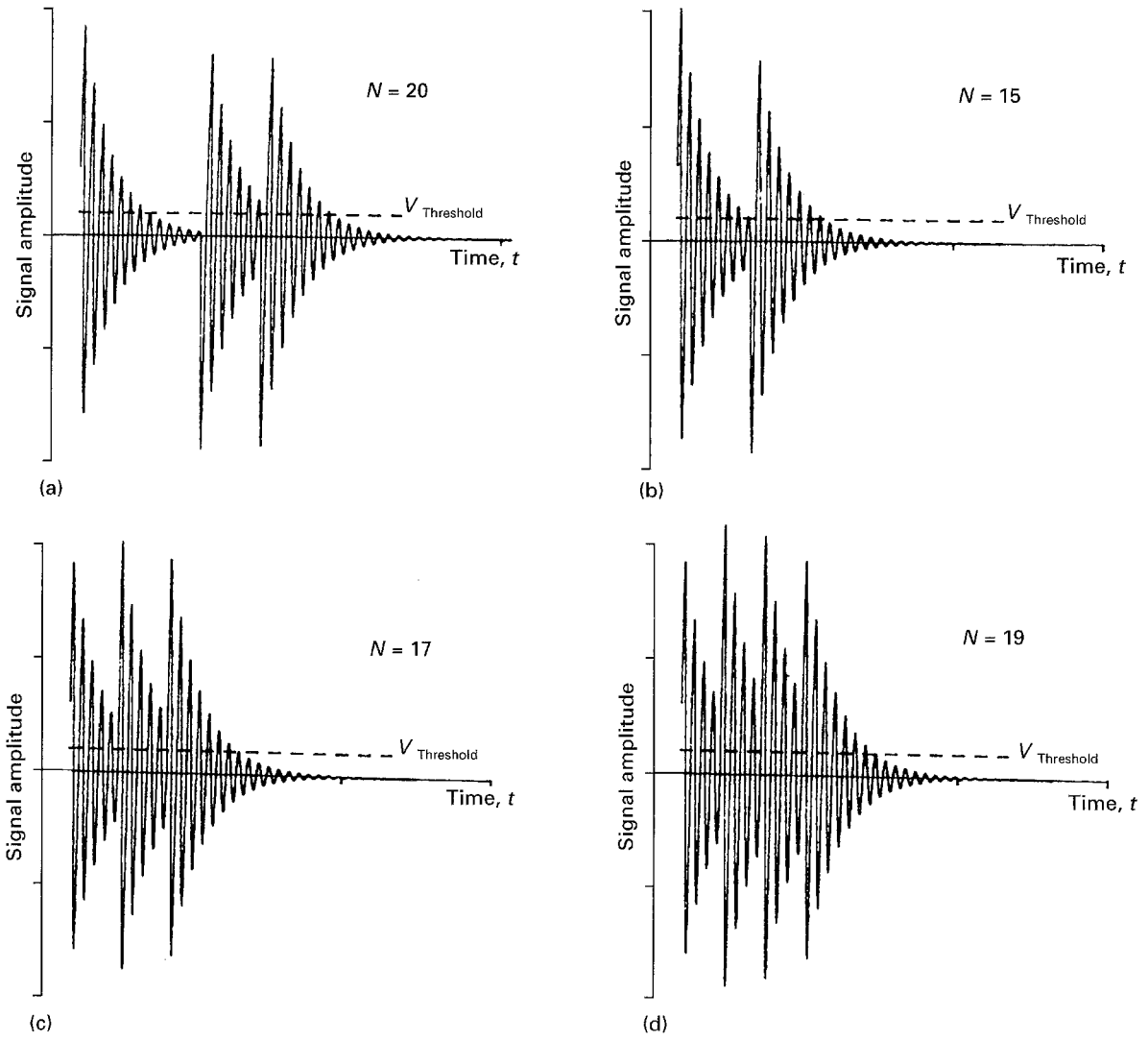


*Figure 8* Schematic AE ringdown signals illustrating (a) possible signal overlap between a single-pulse event and a doublet and comparing possible ringdown counts from (b) doublets, (c) triplets, and (d) quadruplets, with increasing signal overlap.

(a) high AE signal overlap due to the high fibre failure rate in this strain region, and a lack of increase in the count recorded. These signals would constitute lost fibre break signals;

(b) increasing attenuation of the acoustic signal in the test bundle due to a population of fibres already broken.

The possible effects of these factors are shown schematically in Fig. 8. Fig. 8a illustrates the case for signal overlap involving signals from a singlet (first decaying signal) and a doublet. Here, it is clear that lack of signal overlap gives an $N_e$ of about 20 due to the combination of ringdown counts from both signals, as long as the time period separating the last oscillation of the singlet from the first oscillation of the doublet (defined by the threshold) is less than 200 μs. This signal is effectively processed as a "singlet". Fig. 8b–d show doublet, triplet and quadruplet signals, respectively. These illustrate the case of reducing the time, $\Delta t$, separating the individual signals that constitute the multiplet as the multiplet order increases. The effect of this reducing time separation is clear: the ringdown counts from the doublet ($N = 15$), the triplet ($N = 17$) and the quadruplet ($N = 19$) do not vary much compared to the initial count for the resolved signals, because increasing multiplet value is counteracted by signal overlap effects in the cases presented. In fact, the experimentally observed event duration time for these types of fibre failure mode did not show significant variations, which indicates that the $\Delta t$ must be decreasing as multiplet fibre failure order rises. In considering these efects, note that the definition of a multiplet here is different from that of multiplets detected experimentally because in the cases shown in Fig. 8a–c, all these events would be recorded as singlets by the experimental system as they are not resolved in time. Effectively, these multiplets would constitute lost fibre failures which contribute to the saturation of $N_e$.

We repeat that these effects might also be explained by increasing fibre bundle acoustic attenuation due to an increasing broken fibre population within the fibre bundle. Neither of these explanations has been conclusively demonstrated, but they do provide an alternative explanation of the saturation of AE experimental data.

## 5. Conclusion

The non-linear Weibull plots deduced from dynamic tensile testing of fibre bundles is a consequence of the constant crosshead speed mechanical test method used in testing fibre bundles. Continuous dynamic tensile testing of a fibre bundle is a faster method of determining the fibre strength distribution parameters when compared to most other techniques. The method, however, leads to large load drops at high strains, and consequently the Weibull plots are steeper in this strain region.

AE monitoring of the fibre bundles during testing, enabled us to follow the fibre failure events in the bundle, and hence establish the origin of the non-linearity of the Weibull plots. Such plots deduced from the AE event–strain responses of the fibre bundles, shadowed closely those obtained from the tensile stress–strain responses, indicating clearly that the AE output, to a large extent, followed the fibre failure events in the bundle.

Analysis of the AE event output, showed that the singlet fibre failure mode was predominant at low strains, while at high strains various multiplet order fibre failure modes were in operation, consistent with the large load drops within the same strain region of the stress–strain curves. This allowed us to associate the low strain slope, $m_1$, obtained from the Weibull plots, with the dominant singlet fibre failure mode. The steeper slope, $m_i$, at high strains was associated with the multiplet fibre failure modes, where each mode contributed towards the combined plot which effectively combined the slopes of the corresponding multiple of $m_1$.

Attempts to simulate the fibre bundle stress–strain response, have revealed the significant role played by the various fibre failure modes in defining the shape of the stress–strain curve, particularly about and beyond the maximum stress position. This, apart from demonstrating the inadequacy of the two-parameter Weibull treatment, which is valid only when singlet fibre failures are dominant, also questions the validity of the underlying hypothesis of equal load sharing in any configuration of failed and surviving fibres in the bundle with respect to the prevailing test conditions. On the latter issue, a dynamic test at constant crosshead speed, as reported here, would most probably lead to unequal redistribution of load among the surviving fibres in the bundle. Therefore, at high strains, there would be enhancement of the multiplet fibre failure modes due to fewer fibres carrying the excess load and, consequently, a multiplicity of effective Weibull shape parameters which a two-parameter treatment cannot accommodate.

These results obtained in the course of our investigations clearly show that it is not necessary to employ time-consuming methods that give singlet fibre failure mode only, in order to determine the Weibull shape parameter, $m$. Rather, this parameter can always be determined from a faster method as long as the fibre failure modes in operation can be identified, and this is easily done using acoustic emission. As an example, the triplet fibre failure mode would result in an effective Weibull shape parameter of $3m$, from which one deduces $m$. For this to be possible, a suitably adjusted AE technique to complement the tensile stress–strain technique, becomes essential. A combination of both techniques allows faster data acquisition and provides accurate and reliable information on the state of the fibre bundle. The load, strain and ringdown counts for each fibre or group of fibres failure event may be obtained and a range of statistical data may be extracted.

This study demonstrates that the AE technique can be employed to predict the imminence of failure in a test fibre bundle, by considering the stress corresponding to the first few occurrences of the doublet fibre failure mode as a conservative estimate of the strength of the fibre bundle.

## References


1. A. COWKING, A. ATTOU, A. M. SIDDIQUI, M. A. SWEET and R. HILL, *J. Mater. Sci.* **26** (1991) 1301.
2. M. A. HAMSTAD and R. L. MOORE, *J. Compos. Mater.* **20** (1986) 46.
3. Z. CHI, T-W. CHOU and G. SHEN, *J. Mater. Sci.* **19** (1984) 3319.
4. K. E. EVANS, B. D. CADDOCK and K. L. AINSWORTH, *ibid.* **23** (1988) 2926.
5. M. FUWA, A. R. BUNSELL and B. HARRIS, *J. Phys. D.* **9** (1976) 353.
6. M. G. BADER and A. M. PRIEST, in "Progress in science and engineering of composites", edited by T. Hayashi, K. Kawata and S. Umekawa (Japanese Society for Composite Materials, Tokyo, 1982) p. 1129.
7. W. WEIBULL, *J. Appl. Mech.* **18** (1951) 293.
8. R. HILL and E. U. OKOROAFOR, *Composites* **26** (1995) 10.
9. A. N. NETRAVALI, Z.-F. LI and W. SACHSE, *J. Mater. Sci.* **26** (1991) 363.
10. M. A. HAMSTAD, in "Fundamentals of acoustic-emission" edited by K. Ono (UCLA, California, 1979) Ch. 9, pp. 229–59.
11. A.G. BEATTIE, *J. Acous. Emission* **2** (1983) 95.
12. R. HILL and E. U. OKOROAFOR, *Composites* **25** (1994) 13.
13. C. ZWEBEN and B. W. ROSEN, *J. Mech. Phys. Solids* **18** (1970) 189.
14. S. B. BATDORF, in "Concise encyclopedia of composite materials", edited by A. Kelly (Pergamon Press, Oxford, 1989) pp. 254–61.



*Received 1 December 1994*
*and accepted 22 March 1995*